Bull Earthquake Eng (2011) 9:231–261
DOI 10.1007/s10518-010-9228-0

ORIGINAL RESEARCH PAPER

Analysis of the liquefaction phenomena in the village of Vittorito (L'Aquila)

Paola Monaco · Filippo Santucci de Magistris · Salvatore Grasso · Silvano Marchetti · Michele Maugeri · Gianfranco Totani

Received: 2 April 2010 / Accepted: 15 November 2010 / Published online: 2 December 2010

Abstract This paper describes a case-history of liquefaction occurred near the village of Vittorito after the April 6, 2009 L'Aquila earthquake (moment magnitude $M_w = 6.3$), approximately 45 km far from the epicentre. In the document, first, an estimation of the seismic motion in the area has been made. Thereafter, the performed geotechnical investigation is described, followed by the application of some fast assessment criteria for the occurrence of liquefaction, recently proposed by the new Italian Building Code. A careful assessment of all the parameters involved in conventional Seed and Idriss (1971) liquefaction analyses is considered. The cyclic resistance ratio CRR is evaluated by cone penetration tests CPT and by in situ seismic dilatometer tests SMDT; in the latter case CRR is evaluated by different empirical correlations with shear wave velocity V_s and horizontal stress index K_D. Analytical data confirmed the observed occurrence of the liquefaction in Vittorito, even if the acceleration field in the area, produced by the L'Aquila earthquake, was very low.

P. Monaco · S. Marchetti · G. Totani
Department of Structural, Water and Soil Engineering, University of L'Aquila, Nucleo Industriale di Bazzano Sud- S.P. 37, 67100 Monticchio—L'Aquila, Italy

F. Santucci de Magistris
S.A.V.A. Department, Structural and Geotechnical Dynamics Laboratory–StreGa, University of Molise, via Duca degli Abruzzi, 86039 Termoli, CB, Italy

S. Grasso · M. Maugeri
Department of Civil and Environmental Engineering, University of Catania, Viale Andrea Doria 6, 95125 Catania, Italy

F. Santucci de Magistris (✉)
Engineering Faculty, Structural and Geotechnical Dynamics Lab.–StreGa, University of Molise, via Duca degli Abruzzi, 86039 Termoli, CB, Italy
e-mail: filippo.santucci@unimol.it
URL: http://www.stregadynalab.tk/; http://docenti.unimol.it/index.php?u=filippo.santucci

F. Santucci de Magistris
S.A.V.A. Department, via F. de Sanctis, 86100 Campobasso, Italy

Keywords L'Aquila earthquake · Attenuation relationships · Cone penetration test · Seismic Dilatometer Test · Liquefaction

1 Introduction

On April 6, 2009, an earthquake (local magnitude $M_L = 5.8$; moment magnitude $M_w = 6.3$) hit the city of L'Aquila and the surrounding region. 308 people were killed and approximately 1,500 people were injured due to the collapse of masonry and reinforced concrete buildings; around 65,000 people remained homeless.

Several cases of cracks, displacement in the field and some landslides occurred, while the performance of retaining walls and underground structures was satisfactory (GEER Working Group 2009; Monaco et al. 2010).

Few cases of liquefaction were observed in the area. Aydan et al. (2009) reported about the liquefaction that occurred at the Martini district, close to the epicentral area. In that location, sand boils were observed along the Aterno River in an area located southward of the historical centre of L'Aquila. In addition, at Martini district, many NE-SW trending fractures parallel to the river embankment were created as a result of liquefaction. Sand boiling, as thick as 150 mm, was observed in various locations, together with lateral spreading.

The Authors analysed, instead, evidences of liquefaction near the village of Vittorito, approximately 45 km far from the epicentre of the earthquake. This phenomenon is very interesting due to the relatively limited amount of well documented case-histories of liquefaction in Italy and because of its occurrence relatively far from the epicentre, where direct and indirect effects of the earthquake should have vanished. The latter circumstance locates this specific event at the edge or outside from some of the threshold criteria predicted by the new Italian Technical Code for Constructions (NTC 2008).

In the paper, an estimation of the seismic motion in the area is made, based on data collected by the Italian Strong Motion Accelerometer Network. Then, the geotechnical investigation performed in the area is described, followed by the application of the fast assessment criteria of the occurrence of liquefaction reported in NTC (2008). A careful evaluation of all the parameters involved in conventional Seed and Idriss (1971) liquefaction analyses is considered. The cyclic resistance ratio CRR is evaluated by cone penetration tests CPT and in situ seismic dilatometer tests SMDT; in the latter case CRR is evaluated by different empirical correlations with shear wave velocity V_s and horizontal stress index K_D.

2 The liquefaction phenomena in Vittorito

Vittorito is a small village in the L'Aquila prefecture of around 1,000 inhabitants, located approximately 40 km SE of the city of L'Aquila, at an altitude of about 370 m a.s.l.

The area where liquefaction occurred is in the lower part of the municipality, at an elevation of about 250 m a.s.l., close to the right bank of the Aterno river, where ground surface is relatively flat. The area is utilised for agriculture purposes only and no relevant constructions exist, except for the viaducts of the A25 Torano-Pescara highway that run some hundred meters apart from the liquefaction sites, but which were not damaged during the 2009 L'Aquila earthquake.

Figure 1 shows a zoom of the available geological map of the Vittorito region on a scale 1:50,000. In the area, recent alluvial plain deposits are present. Particularly, the embankments of the Aterno river are constituted by Holocene gravelly-sandy alluvial deposits that include

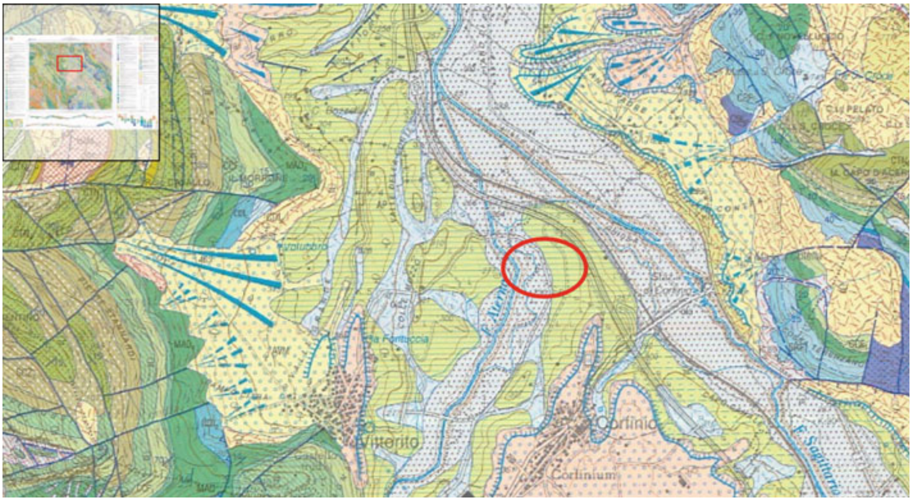

Fig. 1 Geological setting of the village of Vittorito. The red oval indicates the areas where liquefaction phenomena occurred. Main formations: Holocene gravelly-sandy alluvial deposits (*dotted light blue*); Pliocenic-Pleistocenic alluvial deposits (*green-yellow*); Upper Pleistocenic gravelly alluvial deposits (*yellow*); Tortonian marly clayey units (*pink*) (modified after APAT 2010)

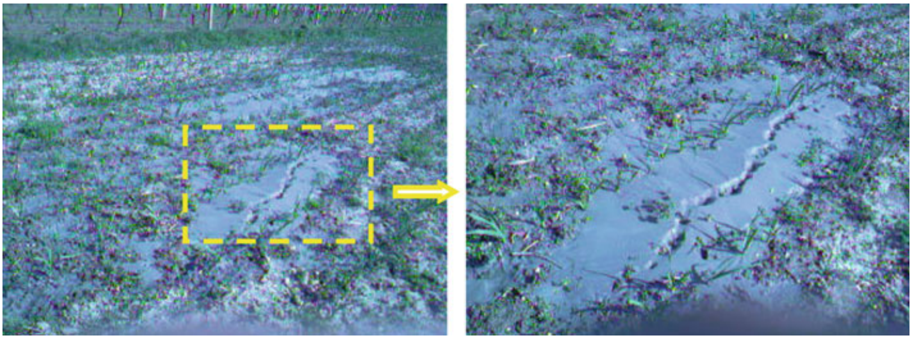

Fig. 2 Outcropping of sand and water as evidence of the liquefaction phenomenon in Vittorito (courtesy of Mr. A. Civitareale)

some silty sand (dotted light blue areas in Fig. 1). Other formations in the geological map (the Anelli-Pescina supersintema) are constituted by Pliocenic-Pleistocenic alluvial deposits composed by coarse-grained materials alternating with coarse debris (green-yellow areas in Fig. 1).

The liquefaction phenomena in Vittorito were revealed through a series of sand boils and sand volcanoes developed in free field during and/or few hours after the main shock of the L'Aquila earthquake.

Available to the Authors, there are a couple of photos made by a local farmer, eye-witnessing that some small sand volcanoes, made of fine-grained sand, appeared in his field in the aftermath of the earthquake (see Fig. 2). Volcanoes were soon flattened fearing that they were an evidence of the ejection of radon, which was considered, in the news, as a strong evidence of a next earthquake.

Local newspapers and internet sites also reported information on this phenomenon. Some referral quotes extracted from Il Centro (2009) indicated that *farmers noticed unusual explosions of bubbles from the ground. Liquefied mud poured out from craters of these mounds. It all happened between Monday 6th and Tuesday 7th, after the earthquake that struck L'Aquila and that was clearly felt in the Valle Peligna. "You know when an anthill is made? The ground was raised and there was a strange slime coming out of the holes. They looked similar to small volcanoes" declared a local farmer. Four or five volcanoes appeared in Le Pietre di Vittorito, about 150 m from the Aterno river (bank towards Corfinio). A member of the technical staff of the municipality confirmed that "There were cracks in the ground three feet long, leaking water mixed with soils. But there is nothing to worry about", while Mr. Giovannitti, mayor of Vittorito says that "As a good fisherman, I recognized in the outcoming soil the material belonging to the Aterno river bed".*

It is worth noticing that during post-earthquake geotechnical investigation at the site, specifically while boreholes were executed, some water and sand was seen moving upwards. This can be interpreted as a minor local liquefaction phenomenon triggered by the vibrations induced by the drilling machines.

3 Ground motion during 2009 L'Aquila earthquake

The April 6th, 2009 01:32:39 GMT L'Aquila earthquake was the strongest event of a sequence that started few months before and lasting for several months after the main shock. It had a Richter magnitude $M_L = 5.8$ and a moment magnitude $M_w = 6.3$. Other two events with magnitude $M_L > 5$ occurred in the following days (April, 7th—$M_L = 5.3$ and April, 9th—$M_L = 5.1$). Up to September 24th, 2009, 31 earthquakes having M_L between 3.5 and 5 occurred (INGV 2009). The distribution of the aftershocks in plan showed very clearly the area affected by the seismic sequence that extends over 30 km in NW-SE, parallel to the axis of the Apennine Mountains (Fig. 3). The sequence of earthquakes occurred mainly in the upper crust at a depth of around 10–12 km from the ground surface. Experimental data correspond to identify the structure responsible for the main shock as a fault with direct movement that stretches for 15 km in NW-SE and immersion SO, whose extension is localized in the surface in agreement to the Paganica fault. According again to INGV (2009), the main shock had the following epicentral coordinates: latitude 42.3476, longitude 13.3800, while the hypocentral depth was estimated at 9.46 km. The focal mechanism shows that the event took place along a normal fault trending NW-SE (strike 147°) with dip SW $< 50°$, as recorded by the Mediterranean Very Broadband Seismic Network (MedNet 2009).

No single recording station of the Italian Strong Motion Accelerometer Network was available in the proximity of the Vittorito area. Maps of the estimated modified Mercalli intensity (Fig. 4a) and of the peak ground acceleration (Fig. 4b) were reproduced on the INGV website in the aftermath of the main shock of the L'Aquila seismic sequence.

The closest seismic station to Vittorito of the Italian Accelerometer Network is the Sulmona digital station that is located 56.4 km away from the epicentre of 2009 L'Aquila earthquake. Figure 5 plots the three components of the Butterworth filtered waveform recorded there for the mainshock, while some relevant synthetic parameters from this motion are reported in Table 1 (both from Working Group ITACA 2010). For these signals, in Fig. 5d, the development of the Arias intensity $I = \pi/2g \int_0^t (a(t))^2\, dt$ normalised to its maximum value $I_A = \pi/2g \int_0^\infty (a(t))^2\, dt$ versus time is also plotted.

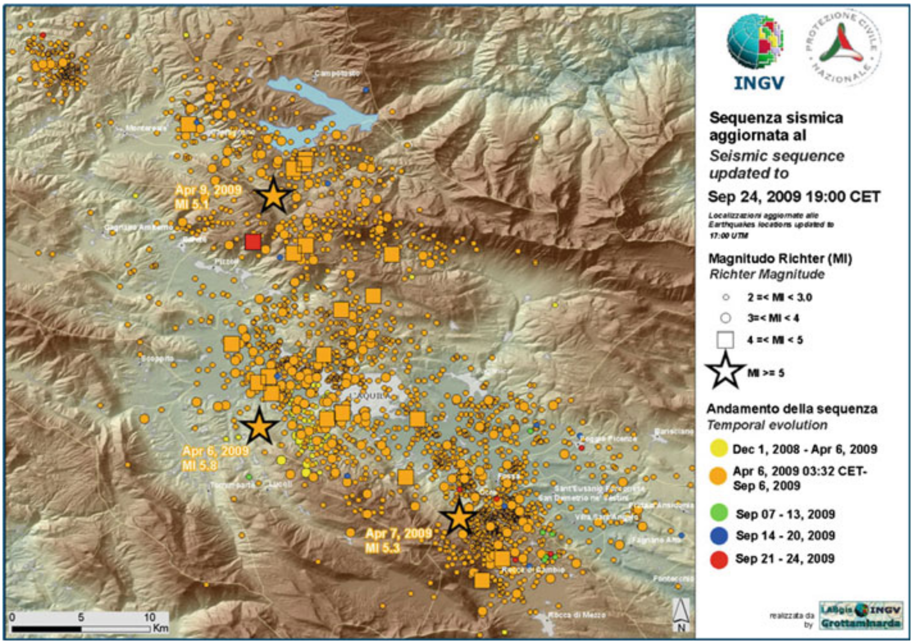

Fig. 3 Epicentral distribution of the L'Aquila sequence until September 24th, 2009 (INGV 2009)

More detailed seismic motion characteristics in Vittorito might be deduced interpolating other available data as published in the Italian strong-motion database.

In Fig. 6a, the peak ground acceleration versus the epicentral distance is reported. Data are distinguished according to the available information on the local geology below the station (Ameri et al. 2009), so that each station could be classified according to the soil categories of Eurocode 8 (EN 1998-1 2004). Notice that none of the stations are placed upon horizontal outcropping bedrock. Hence, some of the data reported here could be influenced by the so-called local effects. Doubts exist for the soil condition below some seismic stations; in this case the subsoils are marked as *not classified* (NC in Fig. 6a).

The same data set is presented in Fig. 6b. In this case, the decay with the epicentral distance of the three components of the motion and of the sole horizontal component, i.e. the vector sum of the East-West and the North-South recordings, is reported. No significant differences could be noticed in the shape of the peak acceleration vs. the epicentral distance relationship for the different components of the motion. Moreover, by Santucci de Magistris and Evangelista (2010), peak vertical-to horizontal acceleration ratio slightly decreases with distance.

From the available data, a maximum horizontal peak ground acceleration PGA of 0.065 g could be estimated on outcropping bedrock for the area of Vittorito.

As underlined by other researchers (e.g. WG UNISANNIO—CIMA—DIGA 2009), a standard attenuation law for the peak ground acceleration employed in Italy (i.e. the Sabetta and Pugliese 1987 relationship) underestimates the recorded accelerations near the epicentral area. Conversely, it overestimates their values away from an approximate epicentral distance of 20 km. This statement can be verified comparing the recorded data with the Sabetta and Pugliese attenuation relationship of the PGA with the epicentral distance, which is plotted in Fig. 6a for earthquakes having a local magnitude of 5.8 and with reference to stiff soils.

(a)

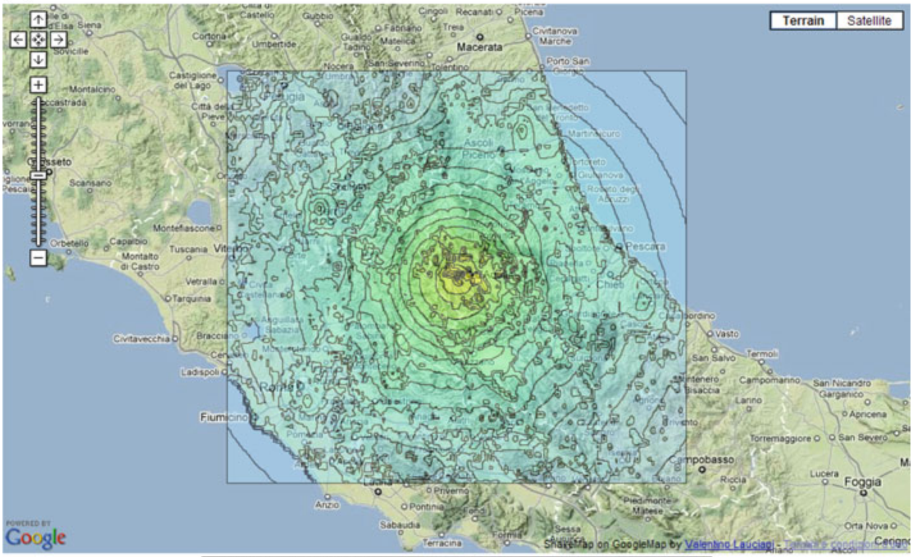

PERCEIVED SHAKING	Not felt	Weak	Light	Moderate	Strong	Very strong	Severe	Violent	Extreme
POTENTIAL DAMAGE	none	none	none	Very light	Light	Moderate	Moderate/Heavy	Heavy	Very Heavy
PEAK ACC.(%g)	<.17	.17-1.4	1.4-3.9	3.9-9.2	9.2-18	18-34	34-65	65-124	>124
PEAK VEL.(cm/s)	<0.1	0.1-1.1	1.1-3.4	3.4-8.1	8.1-16	16-31	31-60	60-116	>116
INSTRUMENTAL INTENSITY	I	II-III	IV	V	VI	VII	VIII	IX	X+

(b)

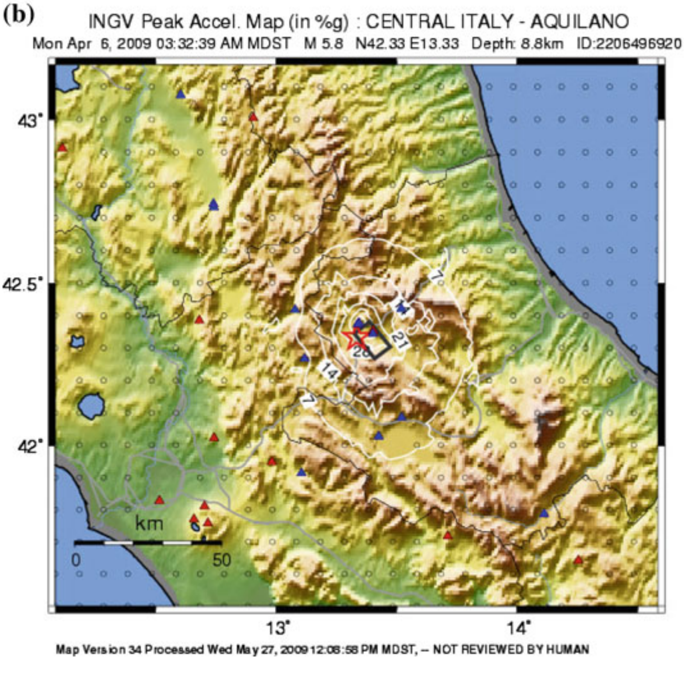

Fig. 4 Shakemaps produced by INGV: (**a**) Modified Mercalli Intensity map and (**b**) Peak ground acceleration (PGA) map for the $M_L = 5.8$ mainshock on 1:32 GMT, April 6th, 2009. *Red triangles*, INGV stations; *Blue triangles*, RAN stations

Fig. 5 Three components of the recording of the April 6th 2009 L'Aquila earthquake mainshock at the Sulmona station and development of the normalized energy of the signals (data from WG ITACA 2010): **a** East-West EW component; **b** North-South NS component; **c** Up-Down UD component; and, **d** development of the normalized Arias intensity with time

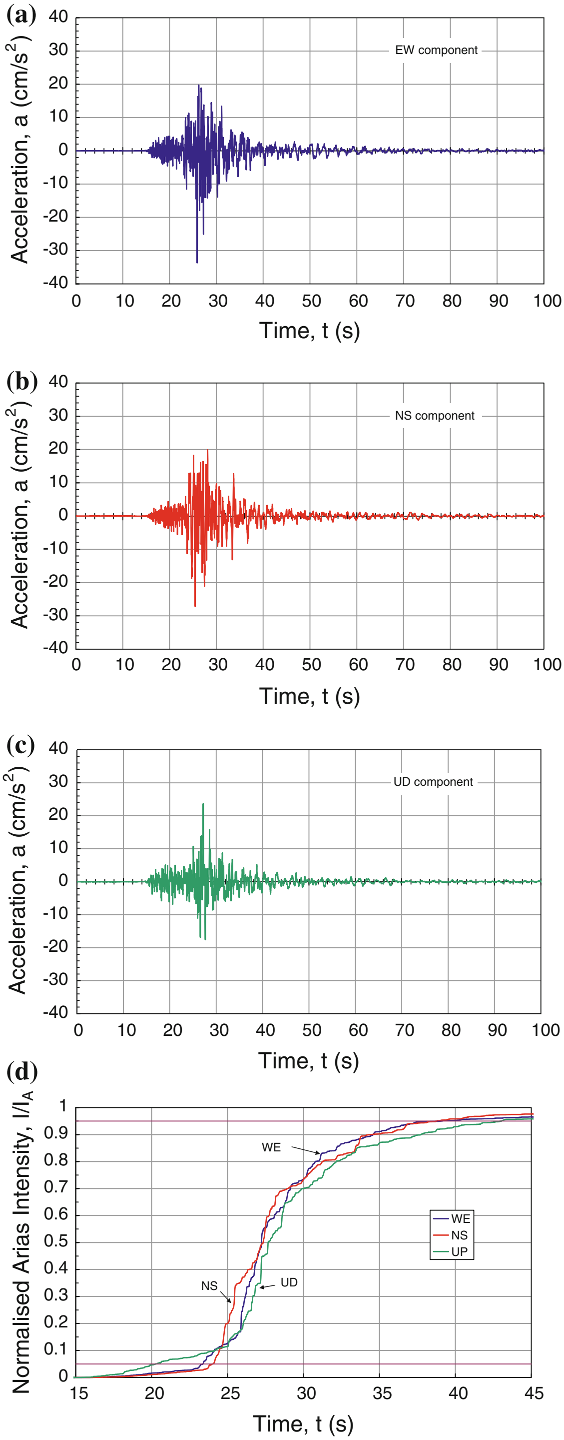

Table 1 Some parameters from the recording of the April 6th 2009 L'Aquila earthquake mainshock at the Sulmona station (data from Working Group ITACA 2010)

	EW	NS	UD
Peak acceleration (cm/s^2)	−27.13	−33.70	23.59
Peak velocity (cm/s)	−3.73	−2.79	−2.45
Peak displacement (cm)	1.23	1.00	0.84
Arias intensity (cm/s)	1.00	0.95	0.49
T90 (s)	14.74	15.64	22.75

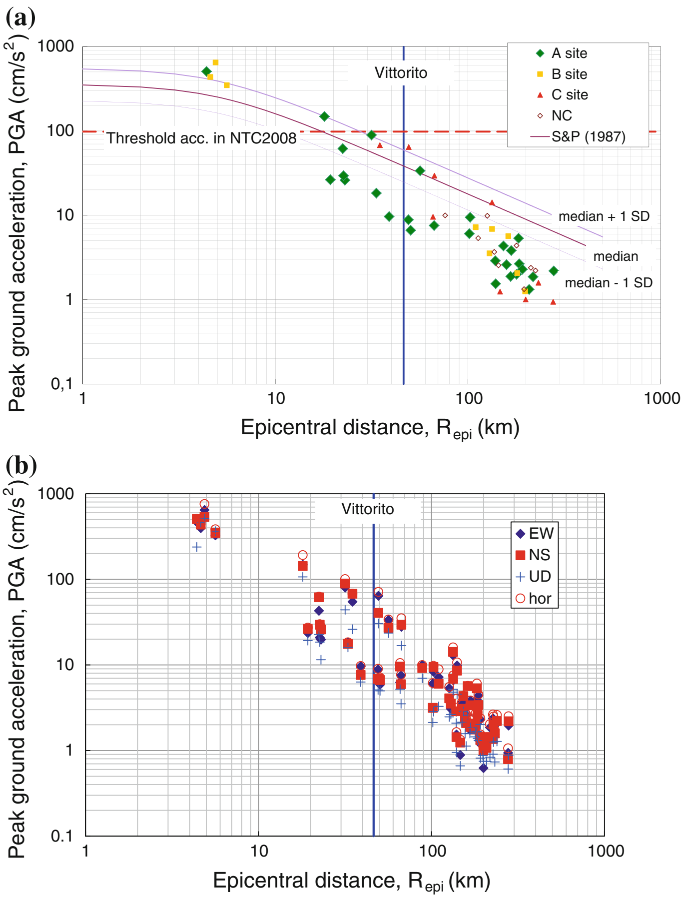

Fig. 6 Attenuation of the peak ground acceleration with the epicentral distance for the April 6th 2009 L'Aquila earthquake: (**a**) data classified according to the ground category below the recording stations compared with the Sabetta and Pugliese (1987) (S&P, 1987) attenuation relationship (average values in *red-violet*, average ± one standard deviation in *light-blue*) and (**b**) attenuation of all the components of the motion

The same consideration applies if other attenuation relationships are employed. For instance, Tropeano and Silvestri, in a personal communication, estimated a mean peak ground acceleration equal to 0.073 g for the area of Vittorito using the Ambraseys et al. (1996)

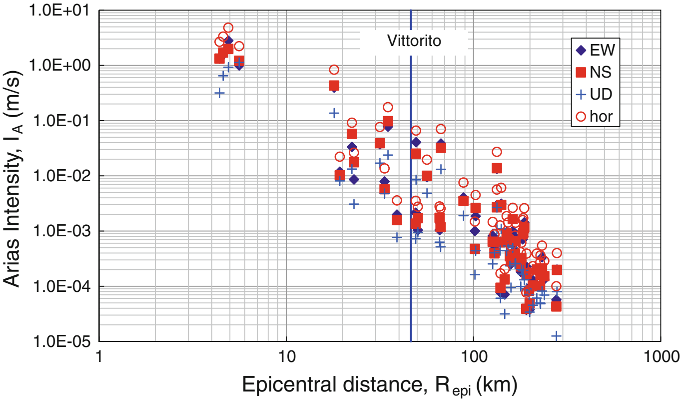

Fig. 7 Attenuation of the Arias intensity with the epicentral distance for the April 6th 2009 L'Aquila earthquake

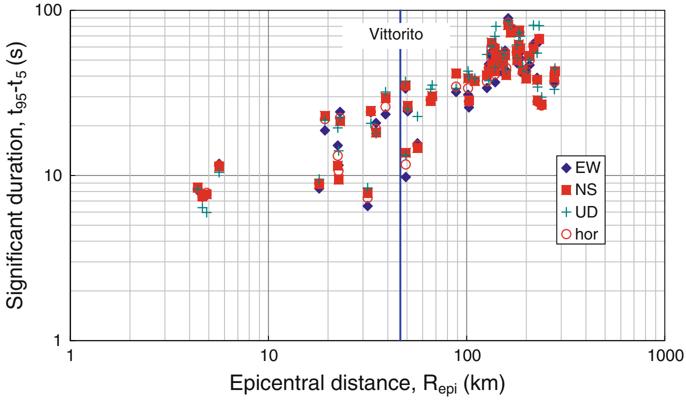

Fig. 8 Increment of the significant duration with the epicentral distance for the April 6th 2009 L'Aquila earthquake

attenuation law, but they noticed that the same formulation overestimates the measured acceleration at the Sulmona recording station. Coherently with the Ambraseys et al. (1996) relationship, they evaluated the site to source distance (i.e., the shortest distance of the site to the surface projection of the rupture surface) according to the Joyner and Boore (1981) formulation. In this case, the fault definition by Cirella et al. (2009) was employed.

The overall motion in the Vittorito area was not so strong in any case, as can be seen from Fig. 7, where the decay of the Arias intensity with distance is reported. Its value can be estimated in the order of $1 \cdot 10^{-2}$ m/s, while, again, no large differences can be observed for the different components of the motion (i.e., those obtained from the East-West, the North-South and the Up-Down recorded accelerograms).

An assessment on the duration of earthquake in Vittorito can be made from Fig. 8. In this case, the significant duration is defined, for each accelerogram, as the time interval between the instants at which the 5 and 95% of the total energy was reached (Trifunac and Brady 1975, see also Fig. 5). An approximate significant duration of about 20 s can be expected at the potentially liquefied sites.

Fig. 9 Location of tests in the area of Vittorito to analyse the occurrence of liquefaction (BH = borehole; SDMT = seismic dilatometer test; CPT = cone penetration test)

4 Geotechnical investigations

A geotechnical investigation was conducted at different sites within a small area where the liquefaction phenomenon was observed. Particularly, two shallow boreholes BH were executed (from the extracted samples, the grading curves of some of the materials were detected), three in situ seismic dilatometer tests SDMT and one cone penetration test CPT were carried out to analyse the soil resistance to liquefaction. The location of the tests is reported in Fig. 9.

Stratigraphic logs, having an overall length of about 5 m, show that in the area the subsoil profile is comprised of an upper layer of vegetable soil having a thickness of about 1 m. This stratum lies above a sandy silt layer having a thickness of about 2 m below which some gravelly materials, with various degrees of cementation, were found. Therefore, it appears that in the first few meters of subsoil, the average particle size of the material increases with depth.

Water table is located at about $0.3 \div 0.5$ m below the ground level.

Figure 10 shows the available grading curves for the shallow materials. Two main soil formations are observed: sandy silt and gravelly sand. The former was found at a depth lower than 1.7 m (tests S1-1, S1-2, S2-2), the latter at a larger depth (tests S1-3, S2-3, S2-4). In both cases, the uniformity coefficient of the materials is relatively high (i.e., soil particle sizes cover a large range).

Figure 11 summarizes the results of the three seismic dilatometer tests that were executed in the area. The flat dilatometer test is a very comprehensive in situ testing technique able to detecting detailed information on soil properties and their variation with depth. Readers might refer to ISSMGE, TC16 (2001) for a detailed explanation on the parameters that can be obtained with this testing procedure, their engineering significance and their limits.

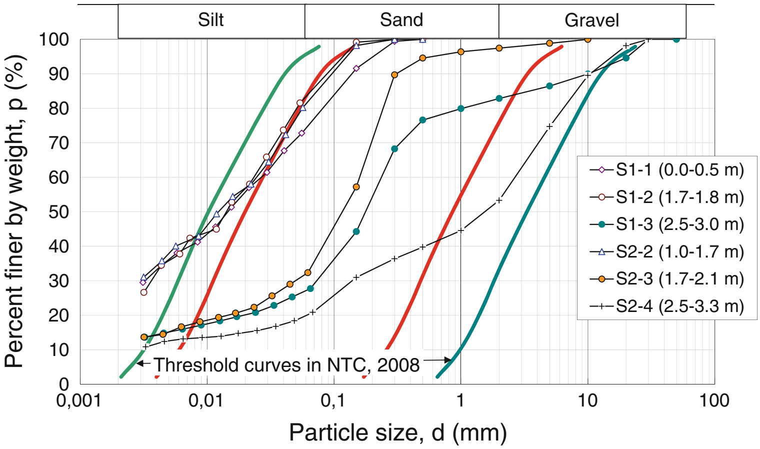

Fig. 10 Grading curves of some materials in the potentially liquefied area and limit curves for a preliminary screening of the liquefaction potential for soil (see Fig. 13) with high coefficient of uniformity as in NTC (2008). The depth of the sample for each borehole is given in the legend

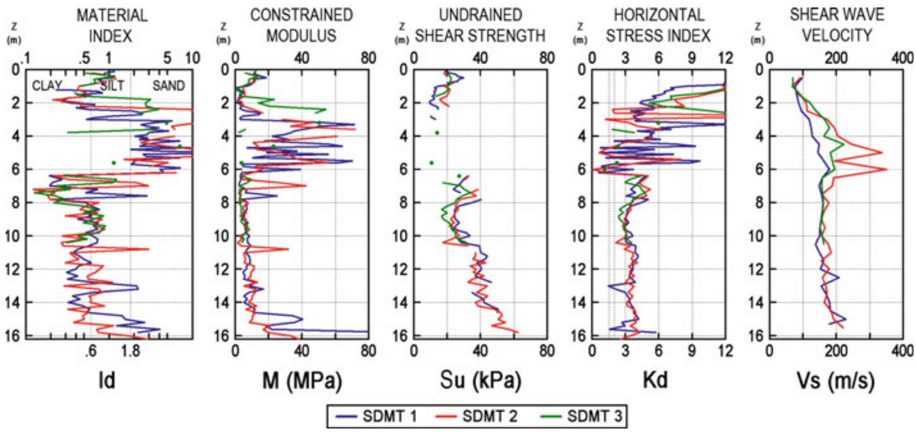

Fig. 11 Results of three Seismic Dilatometer tests in the area of Vittorito

The equipment was recently improved with a seismic module, allowing obtaining reliable shear wave velocity profiles using a kind of double receiver down-hole technique (Marchetti et al. 2008).

The SDMT output in Fig. 11 displays the profile of the shear wave velocity V_s as well as the profiles of four basic DMT parameters—the material index I_D (soil type), the constrained modulus M, the undrained shear strength s_u and the horizontal stress index K_D (related to OCR)—obtained using current DMT correlations (see ISSMGE, TC16 2001, Table 1).

The above parameters are obtained from the two DMT pressure readings: p_0 = pressure necessary to balance the soil pressure and start the movement of the membrane, and p_1 = pressure necessary to move the center of the membrane 1.1 mm against the soil. The material index $I_D = (p_1 - p_0)/(p_0 - u_0)$ provides information on soil type—sand, silt, clay (u_0 = pre-insertion in situ pore pressure). The horizontal stress index $K_D = (p_0 - u_0)/\sigma'_{v0}$ is related to stress history (σ'_{v0} = pre-insertion in situ overburden stress). The profile of K_D

is similar in shape to the profile of the overconsolidation ratio OCR. In clays $K_D \approx 2$ indicates OCR $= 1$, $K_D > 2$ indicates overconsolidation. The constrained modulus M (vertical drained confined 1-D tangent modulus at σ'_{v0}) is obtained as $M = R_M E_D$, where $E_D = 34.7\,(p_1 - p_0)$ is the dilatometer modulus, derived by simple theory of elasticity, and $R_M = f\,(I_D, K_D)$ is a correction factor introduced to take into account overconsolidation and possible high lateral stresses (incorporated via K_D), that reduce considerably soil compressibility. The undrained shear strength in clays is obtained as $s_u = 0.22\,\sigma'_{v0}\,(0.5\,K_D)^{1.25}$.

From Fig. 11, it appears that the soil profiles are almost similar at the three locations where the tests are performed. At a first glance, it also appears that, excluding the gravelly strata from approximately 3 to 6 m below the ground level, the mechanical properties of the soil are relatively poor.

Figure 12 shows the results of the cone penetration test, CPT. Data were obtained using a standard penetration apparatus with a maximum penetration force of 200 kN. The test was terminated at a depth of about 7 m from the ground level, due to the attainment of the maximum loading capability of the device. Above that depth, the soil shows a very low penetration resistance at the cone tip q_c in the first couple of meters, while q_c is relatively higher between 3 and 7 m below the ground level.

The same figure also depicts some physical and mechanical characteristics of the subsoil, as directly derived from the CPT interpretation. Particularly, from the knowledge of the sleeve resistance f_s, the friction ratio profile f_s/q_c is reported. This ratio is higher in the first couple of meters and then it decreases at larger depth. The relative density profile and the effective friction angle profile are also plotted. Relative density is obtained employing both the Harman (1976) and Jamiolkowski et al. (2001) relationships, while the effective friction angle is calculated from q_c using both the Caquot (1934) and the Kulhawy and Mayne (1990) correlations. From the latter diagrams it appears that a loose shallow layer of sand having poor mechanical properties, approximately two meters thick, is followed by a subsequent portion of a soil having better geotechnical characteristics.

5 Fast assessment of liquefaction according to NTC 2008

The new Italian Technical Code for Constructions (NTC 2008) includes specific requirements to exclude the liquefaction phenomenon, modifying an approach already reported in Eurocode 8 (EN 1998-1 2004). Such requirements are related both to the expected seismicity in the area and to the characteristics of the subsoil. The Italian Code asserts that it is possible to skip the verification when at least one of the following circumstances occur:

1. Moment magnitude M_w of the expected earthquake lower than 5;
2. Maximum expected horizontal acceleration at the ground level, in free-field conditions, lower than 0.1 g;
3. Seasonal average depth of groundwater larger than 15 m below the ground level, for sub-horizontal ground and structures with shallow foundations;
4. Subsoil constituted by clean sands having normalized penetrometer resistance $(N_1)_{60} > 30$ or $q_{c1N} > 180$, where $(N_1)_{60}$ and q_{c1N} are respectively the blow count from SPT and the CPT cone resistance, normalized to a vertical effective stress of 100 kPa; and,
5. Grading curve distribution external to some specific areas for soils having a uniformity coefficient $U_c < 3.5$ (Fig. 13a) and for soils having $U_c > 3.5$ (Fig. 13b).

Santucci de Magistris (2006) explains in detail the technical motivations behind the choice of such criteria. In this study, the above conditions were checked against a real case of

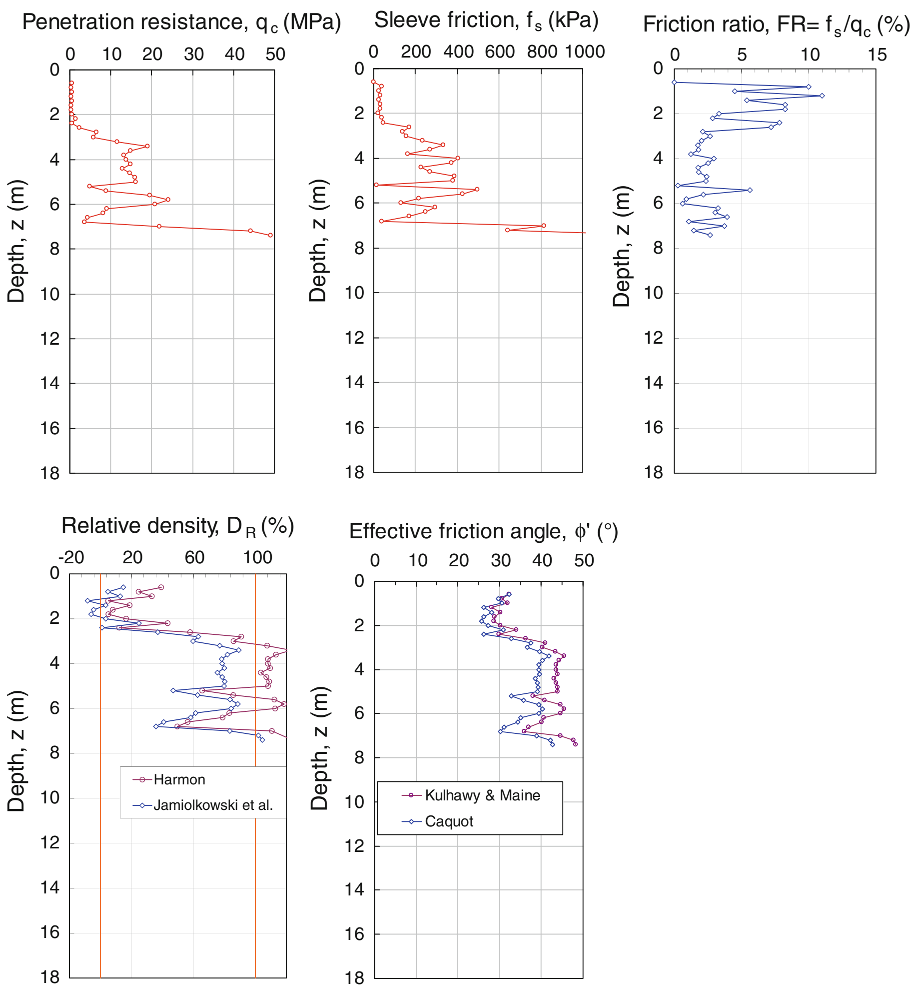

Fig. 12 Data from one Cone Penetration Test in the area of Vittorito and some derived physical and mechanical parameters of the subsoil

liquefaction that occurred in Italy. It can be seen in the following that, based on the available data, the liquefaction case-history at Vittorito is in the borderline or against some of the above listed criteria.

As to points (1) and (3), both the magnitude of the L'Aquila mainshock and the shallow depth of the water table indicate that the occurrence of liquefaction in Vittorito cannot be excluded. Criterion (4) is not employed here, since analyses of the whole investigated profile are performed in the following Sect. 6.

As previously specified, a horizontal peak ground acceleration of 0.065 g was expected on outcropping bedrock in Vittorito. This acceleration is well below the threshold reported in NTC (2008), which was set to 0.1 g. The latter was obtained evaluating, in an approximate way, the peak acceleration at the ground level in correspondence to the minimum value of the cyclic stress ratio CSR in the conventional verification charts.

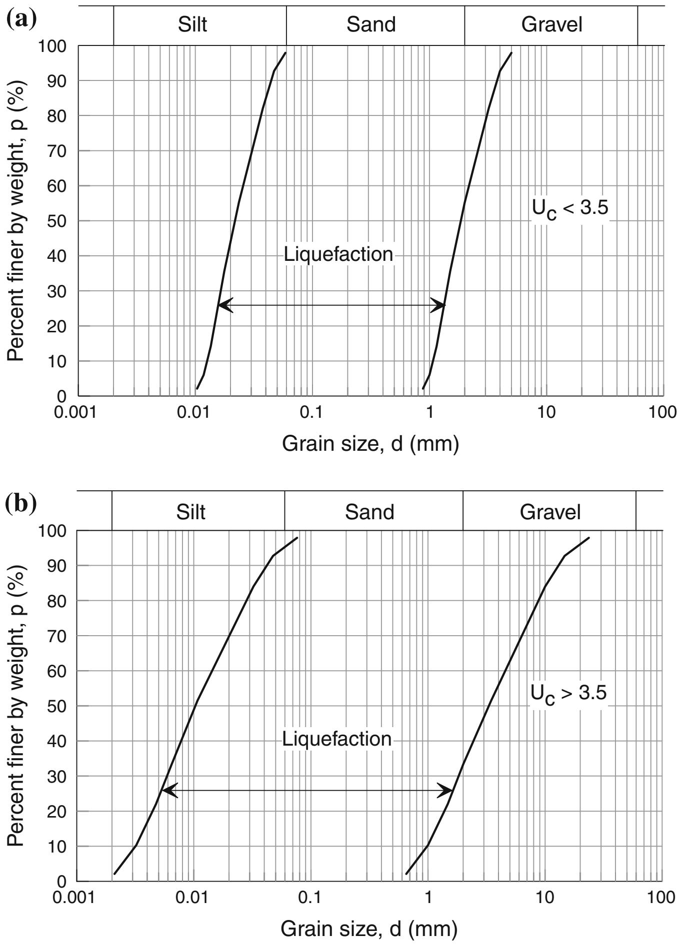

Fig. 13 Grading curves for a preliminary evaluation of the liquefaction potential for soil with low and high coefficient of uniformity (modified after Tsuchida 1970)

Yasuda et al. (2004) indicated evidences of liquefaction in the area of Sapporo for the 2003 Tokachi-oki earthquake in Japan ($M_w = 8.0$). In this zone, that was located more than 200 km away from the epicenter, the measured maximum acceleration was as low as 0.05 g. The threshold was, however, moved upward in NTC (2008) supposing that very low acceleration might cause liquefaction only if generated by ground motions of very long duration (i.e. recorded far from the epicenter and produced from large earthquakes); those are not expected in Italy. As well known, the equivalent number of loading cycles (e.g. Biondi et al. 2004) is another relevant parameter that governs the phenomenon.

This statement is partially confirmed by the analysis of the motion of the Tokachi-oki earthquake as indicated in the next Fig. 14, where the variation of peak ground acceleration, Arias intensity and significant duration are plotted against the epicentral distance. Notice that the data employed here are not affected by site effects due to the peculiar configuration of the Japanese seismic network where, for each station, both data at the surface and well below the ground level are recorded (Okada et al. 2004). The latter, recorded at least at 100 m

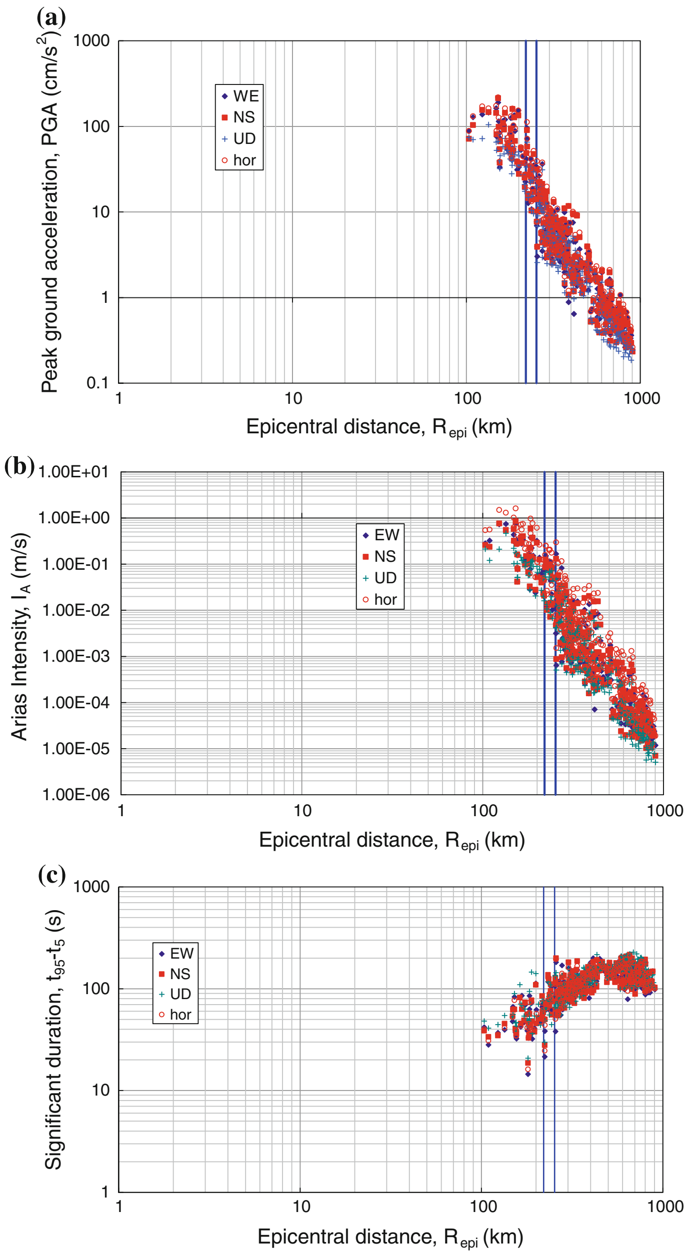

Fig. 14 Variation of the seismic motion with the epicentral distance for the 2003 Tokachi-oki earthquake, Japan: (**a**) peak ground acceleration; (**b**) Arias intensity; and (**c**) significant duration. Blue lines indicate the epicentral distance of the area where liquefaction was observed (data after NEID 2010)

below the ground level, are employed for the plot presented here. It is worth mentioning that the epicenter of this earthquake was 75 km off the Japan coastline and therefore seismic data in the near-field area were not available.

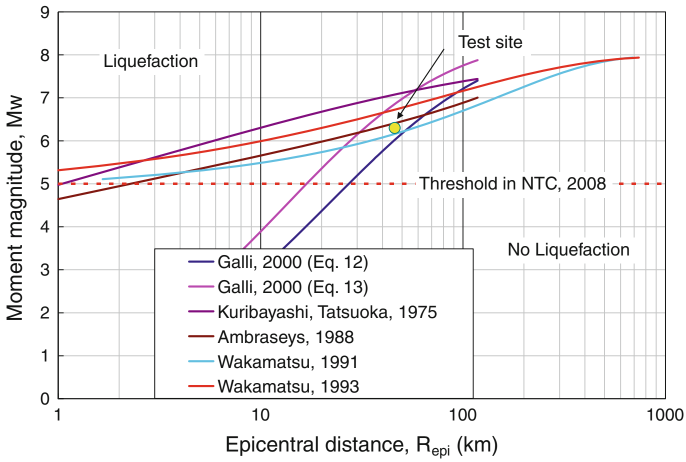

Fig. 15 Magnitude-distance relationship separating liquefaction/non-liquefaction case histories. Point representative of the analyzed case-history is compared with Eqs. 12 and 13 of Galli (2000) and relationships reported in Kuribayashi and Tatsuoka (1975); Ambraseys (1988) and Wakamatsu (1991, 1993)

As a matter of fact, for the sites in northern Japan where liquefaction occurred, Arias intensity was about $1 \cdot 10^{-1}$ m/s and significant duration was about 70–80 s. Then, even though both Vittorito and sites in Japan are placed at the same order of extent of PGA, the characteristics of the motion in the former case are reduced compared with the latter.

Combined information of magnitude and epicentral distance allow assessing the occurrence of liquefaction based on historical evidences. Such criterion is employed, for instance, to assess the maximum extent of a liquefaction susceptible area in Grade-I seismic zonation analysis (ISSMGE, TC4 1999). Some of the literatures evaluating the threshold curves separating liquefaction/non liquefaction case histories are reported in Fig. 15 together with the couple magnitude-epicentral distance for the liquefaction phenomenon in Vittorito.

To construct the graph in Fig. 15, all the data were converted into moment magnitude using Utsu (1982) relationships. It appears again that the situation at the test site is borderline compared with the previously derived relationships, including Equations (12) and (13) of Galli (2000), calibrated entirely on historical Italian data.

Finally, the limit grading curves (Fig. 13) employed to exclude the liquefaction phenomenon developed for harbour structures in Japan (see for instance PIANC 2001) and adopted in the new Italian Building Code (NTC 2008) are reported in the previous illustrated Fig. 10. It appears that, for this specific case, the grading curve distribution does not allow for a-priori exclusion of the liquefaction phenomenon.

6 Assessment of the liquefaction potential using in situ tests

6.1 Procedures of analysis

To verify the possibility of liquefaction occurrence in Vittorito, three simplified procedures were used.

The methods are based on the comparison, at a given depth below the ground level, between the available seismic resistance to liquefaction and the seismic load. Both the parameters are normalized to the current vertical effective geostatic stress to respectively define the non-dimensional cyclic resistance ratio, CRR and the non-dimensional cyclic stress ratio, CSR. If the stress ratio is larger than the resistance ratio liquefaction occurs.

The first procedure, by Andrus and Stokoe (2000) and Andrus et al. (2004), uses the shear wave velocity V_s to detect the soil resistance.

The second is pivoted on the cone penetration test as proposed by Robertson and Wride (1998), and is considered one of the most accurate and complete methodology for the determination of the cyclic resistance profile (Youd et al. 2001). Both CPT-based and V_s-based methods were reviewed by Idriss and Boulanger (2004) and, in this research, the formulation reported in this specific paper is followed.

The third method instead, recently introduced by Monaco et al. (2005), employs the horizontal stress index K_D obtained by the flat dilatometer tests to detect the soil resistance to liquefaction. It is worth noticing that the seismic dilatometer SDMT routinely provides, among other measurements, pairs of profiles of K_D and V_s—both correlated with the liquefaction resistance of sands. Hence, SDMT permits obtaining two parallel independent estimates of liquefaction resistance, one from K_D and the other from V_s, using CRR-K_D and CRR-V_S correlations, in the framework of the commonly used Seed and Idriss (1971) simplified procedure.

As well known, simplified computational methods allow defining the liquefaction safety factor, LSF, through the ratio between the capacity of the soil to resist liquefaction and the seismic demand of the deposit:

$$\mathrm{LSF} = \frac{\mathrm{CRR}}{\mathrm{CSR}} = \left(\frac{\mathrm{CRR}_{7.5}}{\mathrm{CSR}}\right) \cdot \mathrm{MSF} \tag{1}$$

In Eq. (1), $\mathrm{CRR}_{7.5}$ represents the cyclic resistance ratio for an earthquake of magnitude 7.5, CSR is the cyclic stress ratio and MSF is a “Magnitude Scaling Factor”.

The cyclic stress ratio is determined, for the three procedures, by the same relation proposed by Seed and Idriss (1971), while the cyclic resistance ratio is calculated with different formulations, according to the data available from different in situ tests.

The cyclic stress ratio, at one defined depth, is estimated by the following expression:

$$\mathrm{CSR} = \frac{\tau_{\mathrm{average}}}{\sigma'_{v0}} = 0.65 \frac{a_{\max s}}{g} \frac{\sigma_{v0}}{\sigma'_{v0}} r_d \tag{2}$$

where $a_{\max,\,s}$ is the peak ground acceleration at the soil surface; g is the gravitational acceleration, σ_{v0} and σ'_{v0} are, respectively, the total and effective vertical overburden stresses; r_d is a shear stress reduction coefficient of the seismic action that accounts for the deformability of the soil.

$a_{\max,\,s}$ can be obtained by the product of the design ground acceleration a_g for stiff type A ground and a soil factor S, which depends on the subsoil stiffness, often synthesized by an equivalent shear wave velocity $V_{s,30}$ (Eurocode 8, EN 1998-1 2004). Santucci de Magistris (2006) and Santucci de Magistris and Evangelista (2007) discuss on the use of S in Eq. (2). In this research, an arbitrary value $S = 1.35$ is assumed (i.e., the one for ground type D that is constituted by deposits of loose-to-medium cohesionless soil, with or without some soft cohesive layers, in Eurocode 8), the available data not allowing for the direct computation of the site amplification factor.

Following Idriss and Boulanger (2004), the factor r_d in Eq. (2) is:

$$r_d = \exp\left[\left(-1.012 - 1.126\sin\left(\frac{z}{11.73} + 5.133\right)\right) + \left(0.106 + 0.118\sin\left(\frac{z}{11.28} + 5.142\right)\right)\mathrm{M_w}\right] \tag{3}$$

while the Magnitude Scaling Factor in Eq. (1) has the following formulation:

$$\begin{cases} \mathrm{MSF} = 6.9\exp\left(\frac{-\mathrm{M_w}}{4}\right) - 0.058 \\ \mathrm{MSF} \leq 1.8 \end{cases} \tag{4}$$

It can be observed that LSF is computed at one determined depth, while to define the whole liquefaction susceptibility of a site, and mainly to evaluate the potential consequences of the phenomenon, it could be necessary to associate a unique numerical value to the whole LSF profile. A synthetic representative index of the liquefaction susceptivity for a single profile was used in this study. This index, that was introduced by Iwasaki et al. (1982), is the Liquefaction Potential Index $\mathrm{I_L}$, defined as:

$$\mathrm{I_L} = \int_0^{20} \mathrm{F(z)} \cdot \mathrm{w(z)} \cdot dz \tag{5}$$

in which z is the depth from ground level, measured in meters, F(z) is a linear function of the safety factor, that is equal to zero for LSF>1 and to its complement to 1 for LSF < 1, and $\mathrm{w(z)} = 10 - 0.5\mathrm{z}$ is a linear function of z, that decreases with the depth. The values of $\mathrm{I_L}$ vary in an interval from 0 to 100, but the Authors suggest that sites with $\mathrm{I_L}$ values greater than about 15 suffer severe liquefaction effects, whereas effects are minor at sites with a value of $\mathrm{I_L}$ less than about 5. Here, the liquefaction potential index is employed to compare the results of the analytical calculations of the liquefaction susceptibility, reported in the following paragraphs, to the field observation of the phenomenon reported in the previous paragraph.

Youd et al. (2001) compared liquefaction resistance criteria from standard penetration test, SPT, cone penetration test, CPT, shear-wave velocity measurements, $\mathrm{V_s}$, and Becker penetration test, BPT. It was stated that the various field tests provide generally consistent results, no matter which test is applied. They also declared that SPTs and CPTs are generally preferred because of the more extensive databases and past experience, but the other tests may be applied at sites underlain by gravelly sediment or where access by large equipment is limited. On the other hand, Andrus et al. (2004) sustain that the $\mathrm{V_s}$ based CRR curve is more conservative than CRR curves based on other procedures.

As a matter of fact, Idriss and Boulanger (2004) concluded that the practice of using a number of in-situ testing methodologies, as best suited to a particular geologic setting, should continue to be the basis for standard practice, and the allure of relying on a single approach should be avoided. However, employing otherwise the same experimental conditions, different tests show a different sensitivity to the soil relative density that is one of the main factors governing the phenomenon. Specifically, the magnitude of shear wave velocity is less influenced by the soil density as compared to the penetration resistance.

Recent research on seismic dilatometer tests is concentrated on the potentiality of using the DMT horizontal stress index $\mathrm{K_D}$ for liquefaction evaluations. Correlations CRR-$\mathrm{K_D}$ have been developed in the last two decades, stimulated by the recognized sensitivity of $\mathrm{K_D}$ to a number of factors which are known to increase liquefaction resistance (difficult to determine by other tests), such as stress history, prestraining, cementation, structure, and by the

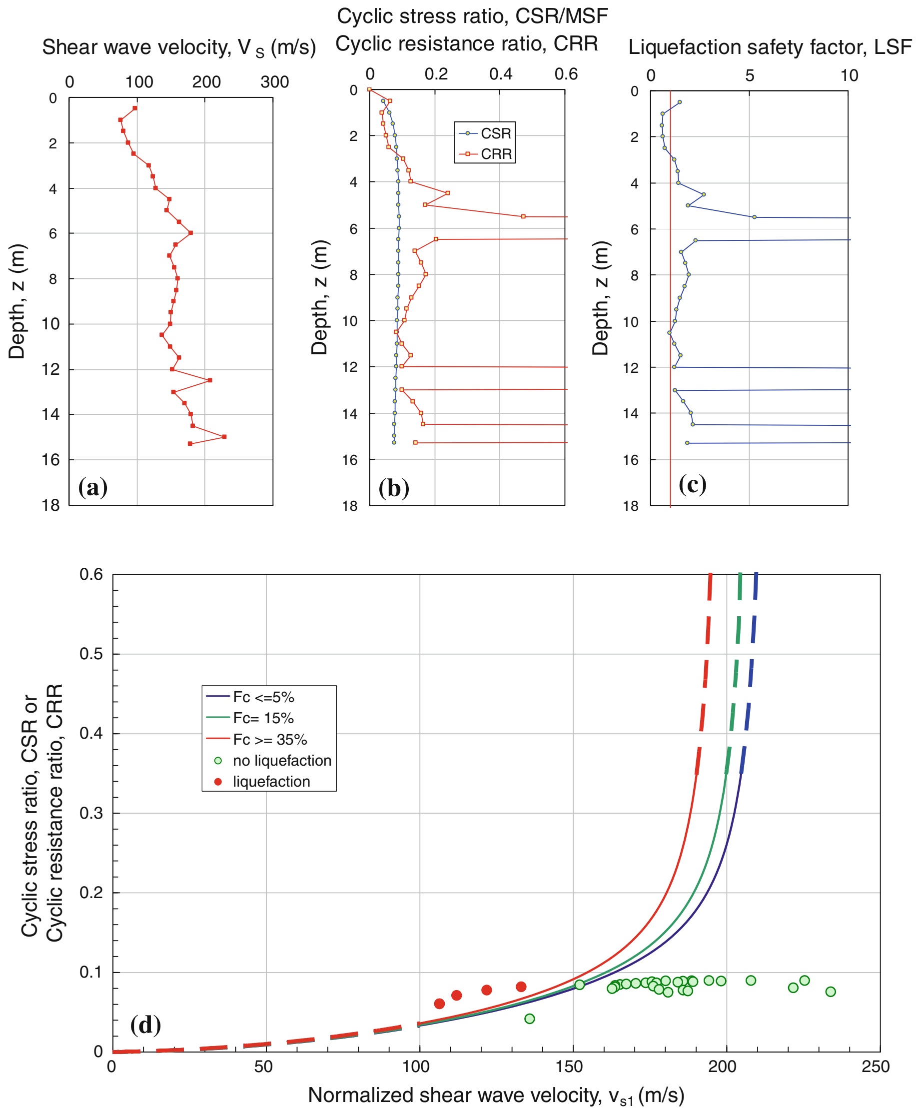

Fig. 16 Example of verification charts using the shear wave velocity from SDMT1: shear wave velocity profile (**a**); cyclic stress ratio and cyclic resistance ratio profiles (**b**); liquefaction safety factor profile (**c**) and liquefaction limit curves (**d**)

relationship of K_D to relative density and state parameter. A key element of the correlation CRR-K_D (Monaco and Schmertmann 2007; Monaco and Marchetti 2007) is the ability of K_D to reflect aging in sands, a factor having a first order of magnitude influence on liquefaction behaviour (see for instance Leon et al. 2006).

A summary of the various correlations developed to estimate CRR from K_D (for magnitude $M = 7.5$ and clean sand) to be used according to the Seed and Idriss (1971) simplified procedure, including the latest CRR-K_D correlation based on all previous data, can be found in Monaco et al. (2005).

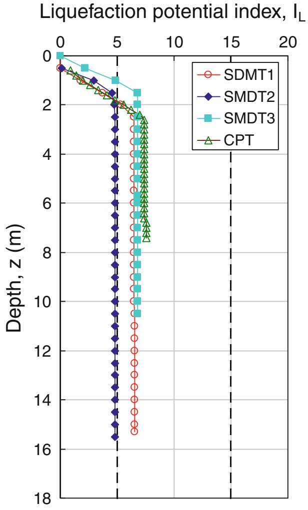

Fig. 17 Liquefaction potential index profiles for the investigated sites in Vittorito, using the shear wave velocity and results of the Cone Penetration Test

Previous comparisons based on parallel measurements of K_D and V_s by SDMT at several sandy sites (Maugeri and Monaco 2006) have indicated that methods based on K_D and V_s often provide substantially different estimates of CRR. Generally CRR from V_s was found to be "more optimistic". This finding opens the question "which CRR should be given greater weight", which is discussed by Maugeri and Monaco (2006) and by Monaco and Marchetti (2007).

6.2 Assessment of the liquefaction potential using the shear wave velocity profiles

As an example, Fig. 16 shows the verification charts obtained using the shear wave velocity profile obtained by SDMT1 (Fig. 16a). Specifically, in Fig. 16b the cyclic stress ratio and the cyclic resistance ratio profiles are reported, while in Fig. 16c depicts the liquefaction safety factor profile. The data are also plotted in Fig. 16d along with the liquefaction limit curves. In the latter case, the red solid symbols indicate the condition of the potential occurrence of the liquefaction phenomenon. It appears that the liquefaction safety factor assumes a value less than one at a depth ranging between 1 and 2.5 m. In this layer, liquefaction is expected to occur. By the way, using shear wave velocity alone is questionable for detecting soil liquefaction (Idriss and Boulanger 2004).

In Fig. 17 the liquefaction potential indices for the three investigated sites, as obtained using the shear wave velocity measurements, are reported. It can be noticed that their values are relatively low, indicating, however, that the potential liquefaction phenomena concentrates only in the top part of the subsoil.

6.3 Assessment of the liquefaction potential using the cone penetration resistance

Verification charts obtained using the Cone Penetration Test data are reported in Fig. 18 using the same type of diagrams as that for the shear wave velocity (i.e., tip resistance in Fig. 18a; cyclic stress ratio and cyclic resistance ratio profiles in Fig. 18b; the liquefaction safety factor profile in Fig. 18c and the liquefaction limit curve in Fig. 18d). It can be observed again that the computed liquefaction safety factors assume values lesser than one in the shallow part of the soil profile, so that the obtained results are very similar to those determined using the

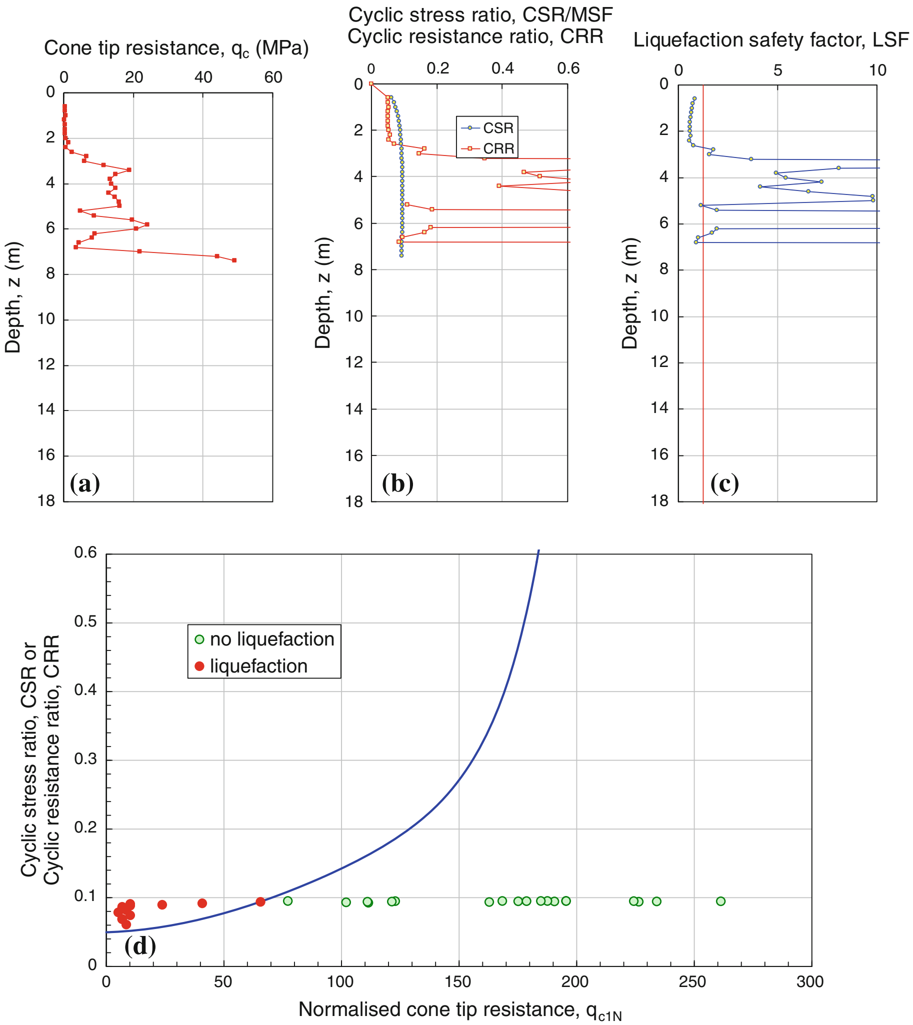

Fig. 18 Verification charts using CPT: cone tip resistance profile (**a**); cyclic stress ratio and cyclic resistance ratio profiles (**b**); liquefaction safety factor profile (**c**) and liquefaction limit curves (**d**)

V_s values. This statement is also confirmed viewing the liquefaction potential index, that assumes a value equal to $I_L = 7.40$ for the soil deposit and that is reported in Fig. 17 along with those obtained from the previously illustrated tests.

It should be noted that the analyses reported herein were performed with the hypothesis that the potentially liquefied material is clean sand. Looking at the grading curves shown in Fig. 10, it is possible to measure a fine content Fc equal to 18%, the fine content being the weight fraction passing through the 200 ASTM sieve (i.e., d = 0.0074 mm). For the shear wave velocity profiles, if the corrections proposed by Andrus and Stokoe (2000) are applied, differences in the liquefaction potential index profiles are negligible (see Fig. 17 compared with Fig. 19, see also Fig. 16d). Rather, the liquefaction safety factor relevantly increases, and the liquefaction potential index decreases, if the CPT data are corrected following the Robertson and Wride (1998) approach. The latter is based on the computation of the soil

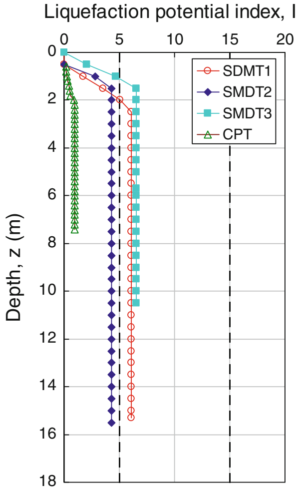

Fig. 19 Liquefaction potential index profiles for the investigated sites in Vittorito using the shear wave velocity from SMDT and the cone penetration resistance from CPT, accounting for the fine content of the materials

behaviour type index I_c that can be calculated based on the cone tip resistance q_c and the sleeve resistance f_s. Differences in the analytical results of the analyses can be re-observed comparing Fig. 17 with Fig. 19, where the liquefaction potential indices, computed by accounting for the fine fraction, are plotted. It should be recalled that, as underlined by Idriss and Boulanger (2004), the use of CPT data alone to determine the grain size characteristics can lead to unreliable results in many cases, particularly while dealing with soils in the transitional range between silty sand and silty clay.

Liquefaction chart and liquefaction safety factor profile using data corrected for the fine content are reported in Fig. 20.

It can be seen that liquefaction could occur at a depth ranging between 1 and 2.5 m from the ground level, where the liquefaction safety factor assumes value lesser than one; also the safety factor is about one at some specific depth between 5 and 6.5 m below the ground level.

6.4 Assessment of the liquefaction potential using the DMT horizontal stress index

At the site of Vittorito, the cyclic stress ratio CSR calculated using Eq. (2) was compared with the cyclic resistance ratio CRR evaluated from K_D according to Monaco et al. (2005):

$$\mathrm{CRR} = 0.0107\,K_D^3 - 0.0741\,K_D^2 + 0.2169\,K_D - 0.1306 \tag{6}$$

Figure 21b shows the comparison of the profiles of CSR and CRR estimated from K_D obtained by SDMT1 (shown in Fig. 21a). Figure 21c shows the corresponding profile of the liquefaction safety factor. The CSR-K_D data points obtained from SDMT1 are also plotted in Fig. 21d together with the liquefaction boundary curve. In this figure the red solid symbols indicate the condition of possible occurrence of liquefaction.

Comparable results have been obtained for SDMT2 and SDMT3 (see profiles of the liquefaction potential index I_L in Fig. 22).

Figure 23 shows a comparison of the liquefaction potential index computed according to Monaco et al. (2005) and that evaluated with the empirical $\mathrm{CRR} - K_D$ correlation reported by Grasso and Maugeri (2006):

$$\mathrm{CRR} = 0.0308\,e^{(0.6054 K_D)} \tag{7}$$

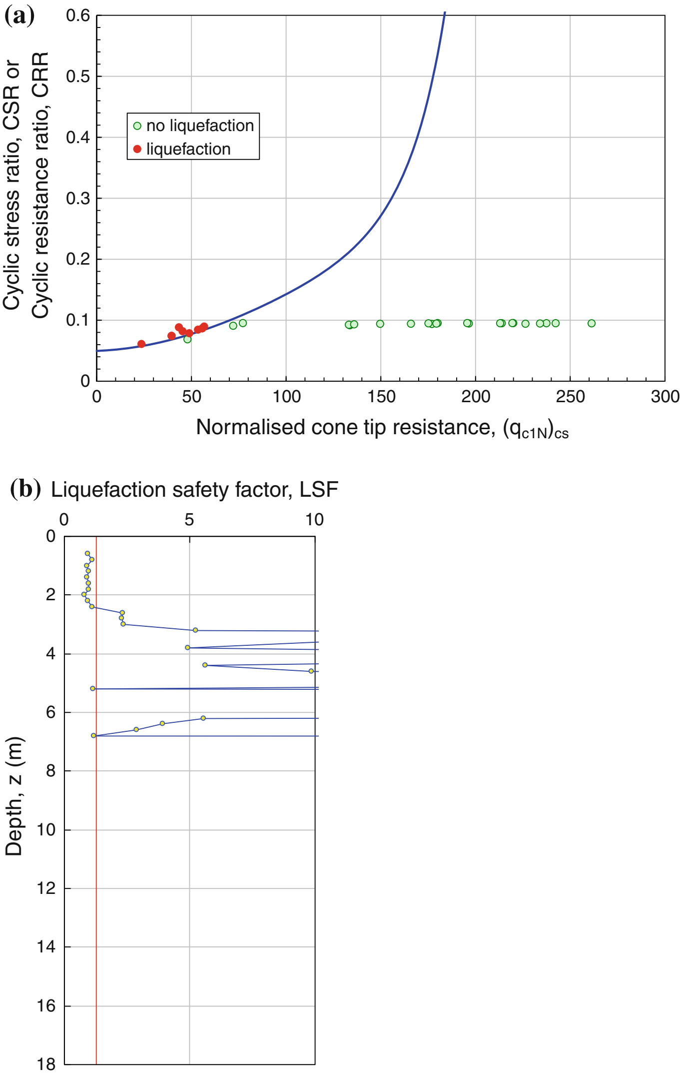

Fig. 20 Verification charts using CPT: liquefaction limit curves (**a**) and liquefaction safety factor profile (**b**), accounting for the fine content of the materials

The Monaco et al. (2005) Eq. (6) was derived considering a generic sandy site, while the Grasso and Maugeri (2006) correlation is related to Catania (Italy) sandy soil along the shore line. For Vittorito site, Fig. 23 shows the liquefaction potential index evaluated by these two approaches: the obtained results show some agreement. However, the liquefaction potential index computed using the Grasso and Maugeri (2006) relationship is in general slight underestimated compared to that evaluated using the Monaco et al. (2005) approach. More in detail, the Liquefaction Potential Index is similar for SDMT1 and SDMT2, where the soil profile is almost comparable, while the soil profile for SDMT3 shows higher values

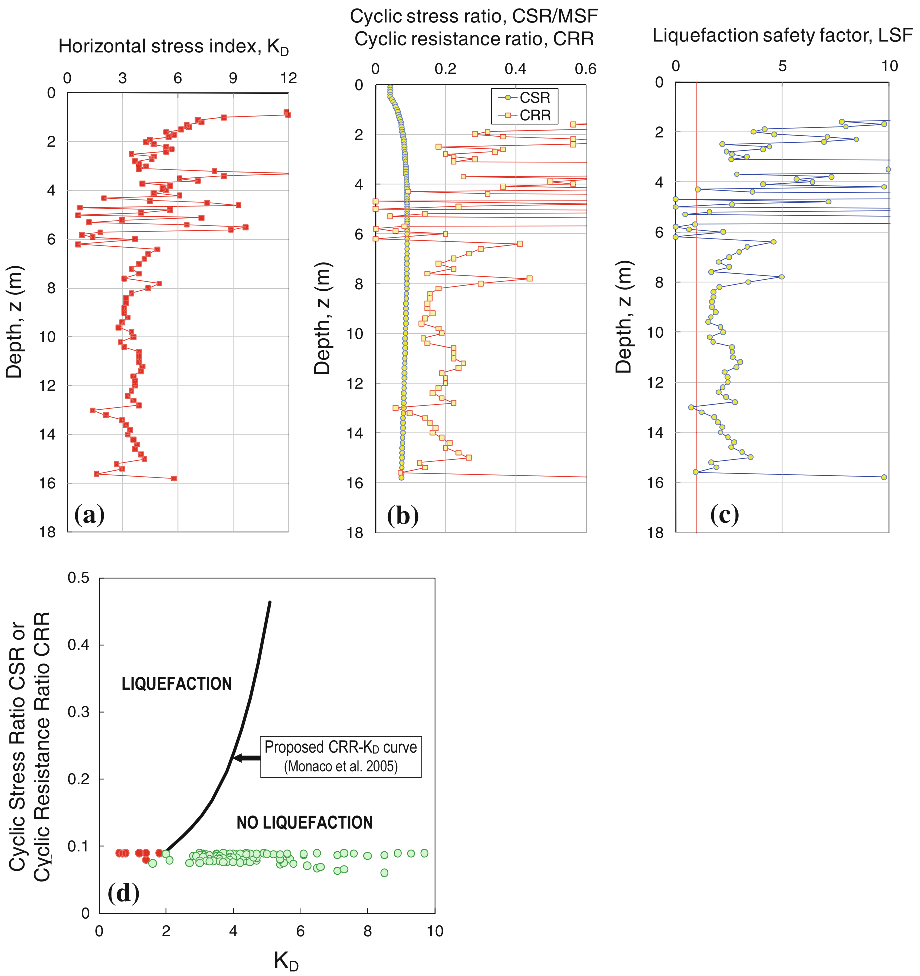

Fig. 21 Example of verification charts using the horizontal stress index from SMDT1: horizontal stress index profile (**a**); cyclic stress ratio and cyclic resistance ratio profiles (**b**); liquefaction safety factor profile (**c**) and liquefaction limit curves (**d**)

of constrained modulus M and higher values of K_D profiles, comparing with the values of SDMT 1 and 2 (Fig. 11).

NTC (2008) proposes new criteria to detect the stratigraphic amplification, compared to those reported in Eurocode 8 (EN 1998-1 2004). Particularly, the formulation incorporates the soil non-linearity to some extent.

Using the maximum proposed amplification factor given by NTC (2008), that is $S = 1.8$ for ground type D, the values of the liquefaction potential index evaluated by Monaco et al. (2005) and evaluated according to the empirical correlation reported by Grasso and Maugeri (2006) are recomputed and reported in Fig. 24. A moderate increase of the liquefaction potential index, ranging between 5 and 10 can be noticed in this case.

Furthermore, even if the peak acceleration estimated at Vittorito for the April 6, 2009 L'Aquila Earthquake is low because of the relatively large epicentral distance, the Italian

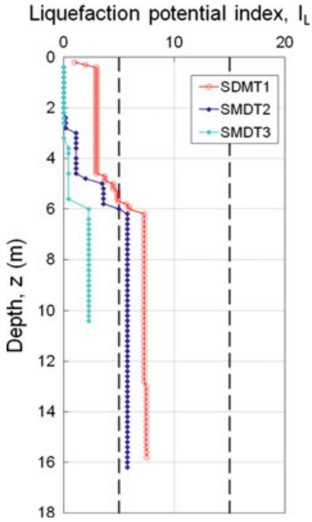

Fig. 22 Liquefaction potential index profiles for the investigated sites in Vittorito using the horizontal stress index from SMDT, according to Monaco et al. (2005)

Technical Code for Constructions (NTC 2008) prescribes for the Vittorito area a PGA equal to 0.257 g with a probability of occurrence of 10% in 50 years (return period $T_R = 475$ years). This is because the main seismic hazard for the area essentially derives from seismogenic sources different from those generating the L'Aquila earthquake and located at a closer distance.

Figure 25 shows the potential liquefaction index computed for a PGA equal to 0.257 g at the bedrock, using the soil amplification factor of 1.49 given by the NTC (2008). The liquefaction potential index evaluated by Monaco et al. (2005) and by Grasso and Maugeri (2006) for all the three SDMT tests is greater than 15, which not only points that liquefaction occurred during the April 6, 2009 L'Aquila earthquake, but also indicates that the liquefaction hazard could be very high in the Vittorito area.

From Figs. 23–25 it can be seen that liquefaction could occur at a depth ranging between 2 and 6 m, where the fine content is at a very low percentage, while in the upper 2 m K_D values are very high, due to the possible presence of more rigid upper crust, so that the CRR values evaluated by K_D are very high; the possible presence of rigid upper crust is in general not felt by V_s profile and not felt enough by tip resistance q_c.

7 Conclusions

The occurrence of liquefaction at the bank of the river Aterno, near the village of Vittorito, is analysed and discussed in this paper. The site is relatively far from the epicentre of the April 6, 2009 L'Aquila earthquake; the estimated seismic actions are relatively low, as confirmed from the limited damages in the area and from the analysis of the recorded accelerometer field.

Among others, fast assessment criteria proposed by the recently introduced Building Code in Italy indicate the possible occurrence of the liquefaction phenomenon when the PGA at the ground level exceeds 0.1 g. The PGA in the Vittorito area, induced by the 2009 L'Aquila earthquake with a considerable epicentral distance of about 45 km, was estimated in 0.065 g

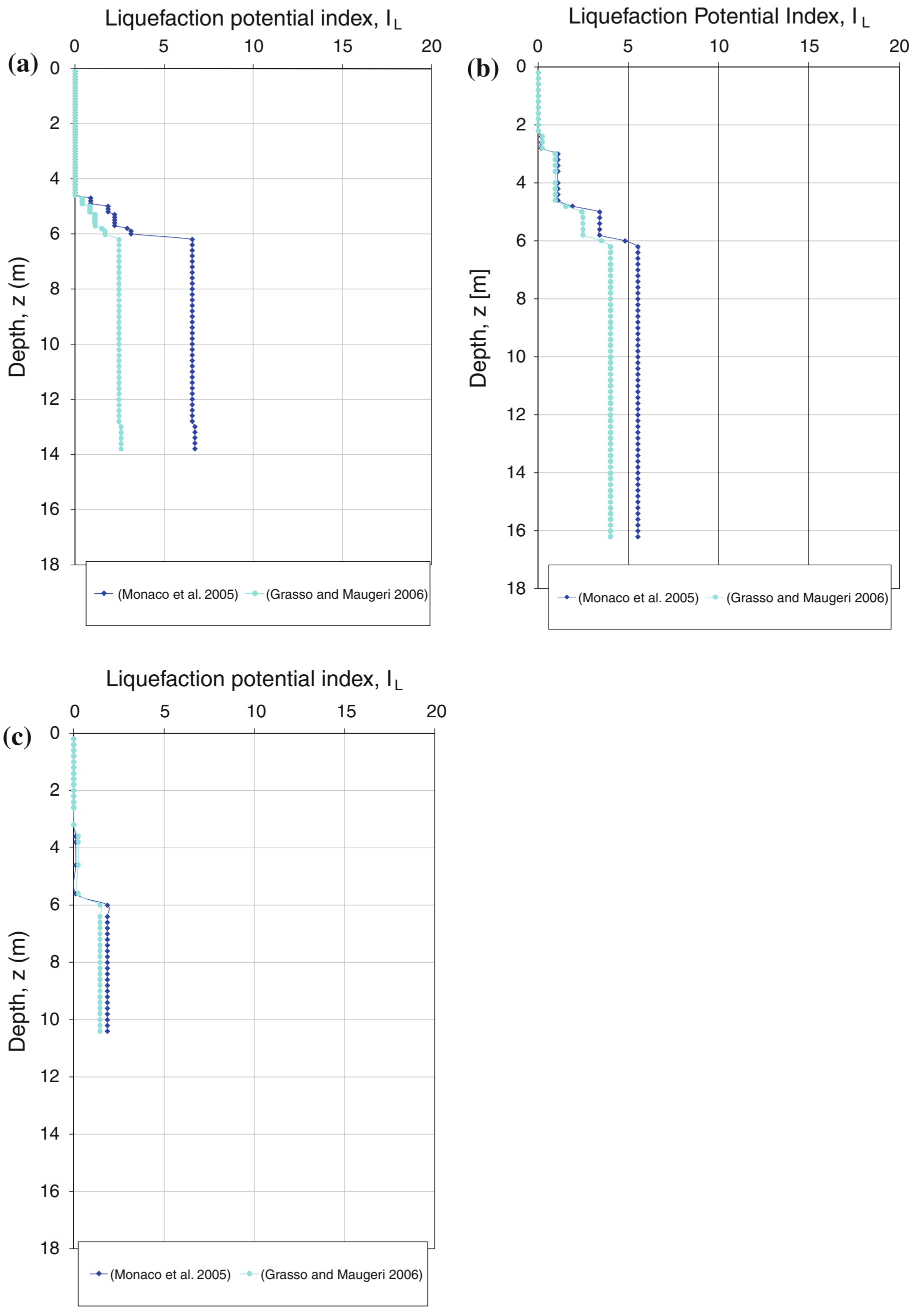

Fig. 23 Liquefaction potential index profiles for the investigated sites in Vittorito using the horizontal stress index from SMDT, according to Grasso and Maugeri (2006): (**a**) SDMT 1; (**b**) SDMT 2; (**c**) SDMT 3

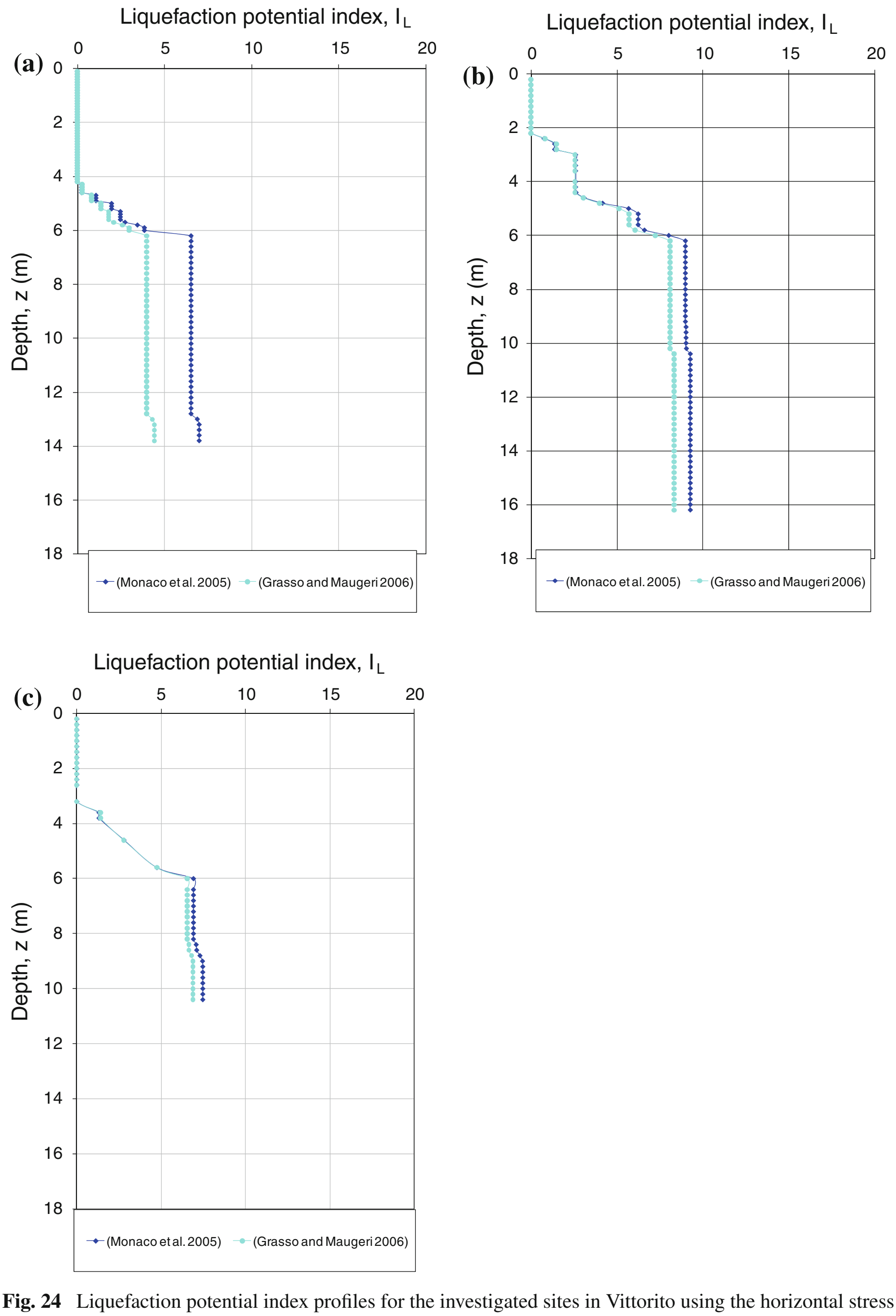

Fig. 24 Liquefaction potential index profiles for the investigated sites in Vittorito using the horizontal stress index from SMDT, according to Grasso and Maugeri (2006) using the amplification factor given by the NTC (2008): (**a**) SDMT 1; (**b**) SDMT 2; (**c**) SDMT 3

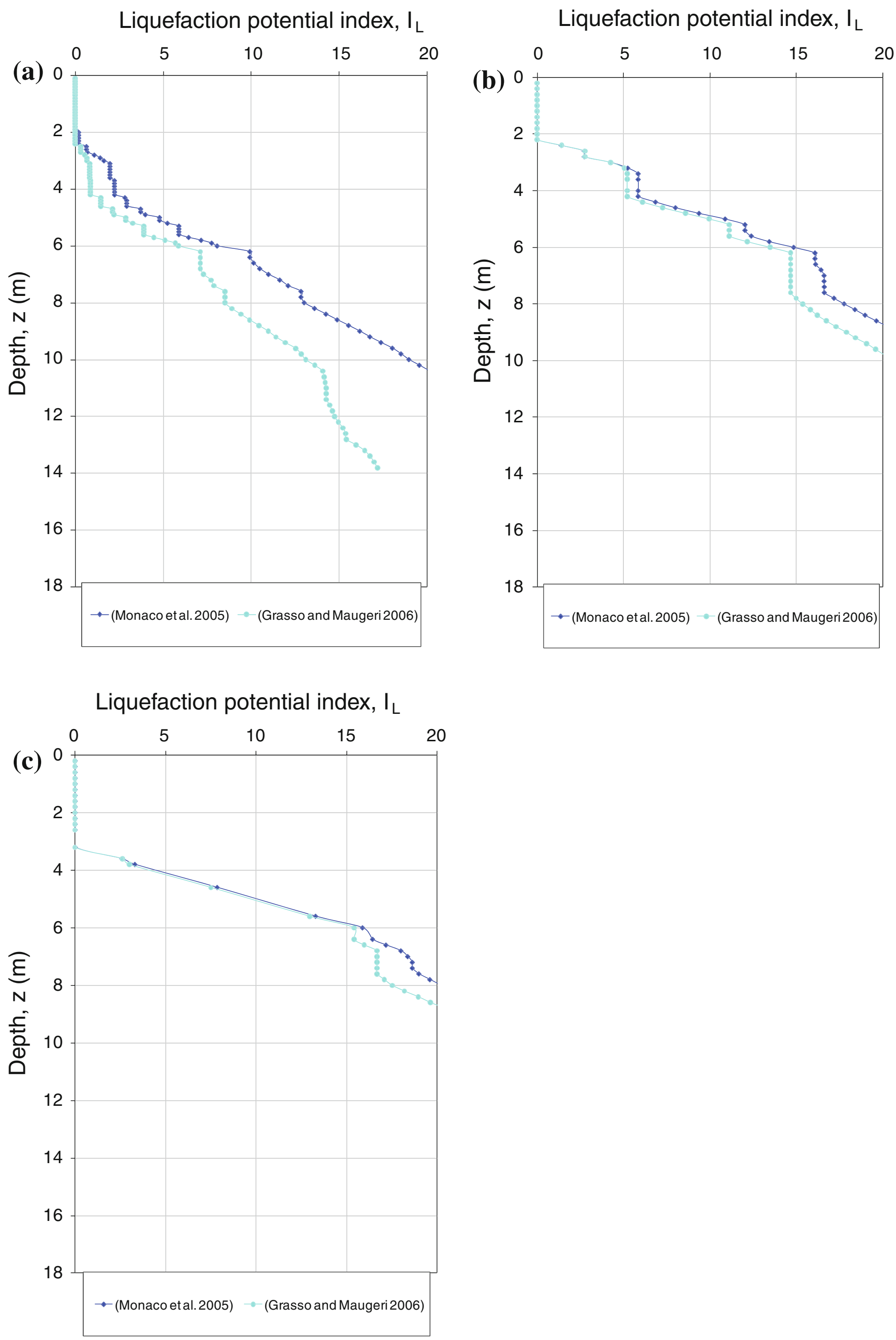

Fig. 25 Liquefaction potential index profiles for the investigated sites in Vittorito using the horizontal stress index from SMDT, according to Grasso and Maugeri (2006) using the acceleration and amplification factor given by the NTC (2008): (**a**) SDMT 1; (**b**) SDMT 2; (**c**) SDMT 3

(less than 0.1 g) at bedrock level, but liquefaction occurred surprisingly and it was analysed in this paper.

The comparison of the profiles of the liquefaction safety factors estimated by different literature methods, where the soil resistance is obtained by measurements of shear wave velocity, V_s, cone resistance, q_c and horizontal stress index from flat dilatometer tests, K_D, suggests that the liquefaction potential index is moderately high. As a matter of fact, the liquefaction occurred at the site of Vittorito, in shallow sand layers of limited thickness, during the April 6, 2009 L'Aquila earthquake. This statement seems to confirm the evidences captured in the aftermath of the 2009 L'Aquila earthquake, according to which some soil volcanoes made by fine sands appeared along the banks of river Aterno in Vittorito.

Two methods, where the soil resistance to liquefaction is evaluated based on shear wave velocity V_s and tip resistance q_c, consistently indicate that possible liquefaction occurred at very shallow depth, at approximately $1 \div 2.5$ m below the ground level, in sandy silts soils.

Liquefaction may have occurred even at a the depth of 2–6 m below the ground level, according to analyses based on horizontal stress index K_D.

In the case of occurrence in Vittorito of a closer earthquake with a PGA equal to 0.257 g and a site amplification $S = 1.49$, according to the Italian Technical Code for Constructions (NTC 2008), the analysis shows that the liquefaction potential index reported in Fig. 25 could be very high, and so the soil liquefaction phenomena can occur even in case future shocks.

Acknowledgments The occurrence of liquefaction at some locations in the area of the village of Vittorito was reported by a personal communication of Dr. Galadini, National Institute of Geophysics and Vulcanology, Italy, whose suggestion was really appreciated. The Authors whish to thank also Mr. Maurizio Calabrese, Ms. Nadia Calandrella, Mr. Angelo Civitareale, Dr. Arindam Dey, Dr. Anna d'Onofrio, Dr. Giovanni Lanzano, Mr. Diego Marchetti, Mr. Alfredo Ponzo, Prof. Francesco Silvestri, Dr. Giuseppe Tropeano for their help in developing this paper.

References

Ambraseys NN (1988) Engineering seismology. Earthq Eng Struct Dyn 17:1–105

Ambraseys NN, Simpson KA, Bommer JJ (1996) Prediction of horizontal response spectra in Europe. Earthq Eng Struct Dyn 25:371–400

Ameri G, Augliera P, Bindi D, D'Alema E, Ladina C, Lovati S, Luzi L, Marzorati S, Massa M, Pacor F, Puglia R (2009) Strong-motion parameters of the $M_W = 6.3$ Abruzzo (Central Italy) earthquake. INGV internal report. http://www.mi.ingv.it/docs/report_RAN_20090406.pdf. Accessed 30 October 2010

Andrus DR, Stokoe KH II (2000) Liquefaction resistance of soils from shear-wave velocity. ASCE J Geotech Geoenviron Eng 126(11):1015–1025

Andrus DR, Stokoe KH II, Juanga H (2004) Guide for shear-wave-based liquefaction potential evaluation. Earthq Spectra 20(2):285–308

APAT (2010) Environment Protection Agency and Technical Service Agency. Carta Geologica d'Italia. Foglio 369 Sulmona. http://www.isprambiente.it/MEDIA/carg/369_SULMONA/Foglio.html. Accessed 30 October 2010

Aydan O, Kumsar H, Toprak S, Barla G (2009) Characteristics of 2009. L'Aquila earthquake with an emphasis on earthquake prediction and geotechnical damage. J Sch Marine Sci Tecnol, Tokai Univ 7(3):23–51

Biondi G, Cascone E, Maugeri M (2004) Number of uniform stress cycles equivalent to seismic loading. In: Doolin et al (ed) Proceedings of 11th ICSDEE & 3rd ICEGE. Berkeley, CA, USA, vol 2, pp 705–712

Caquot A (1934) Equilibre des massiffs à frottement interne. Gauthier Villars, Paris

Cirella A, Piatanesi A, Cocco M, Tinti E, Scognamiglio L, Michelini A, Lomax A, Boschi E (2009) Rupture history of the 2009. L'Aquila (Italy) earthquake from non-linear joint inversion of strong motion and GPS data. Geophy Res Lett 36:L19304

EN 1998-1 (2004) Eurocode 8: design of structures for earthquake resistance—part 1: general rules, seismic actions and rules for buildings. CEN European Committee for Standardization, Bruxelles, Belgium

Galli P (2000) New empirical relationships between magnitude and distance for liquefaction. Tectonophysics 324:169–187

GEER Working Group (2009) Preliminary report on the seismological and geotechnical aspects of the April 6 2009 L'Aquila earthquake in central Italy. Report for web dissemination, geotechnical earthquake engineering reconnaissance GEER Association, Report No. GEER-016, Version 2., May 6, 2009. http://www.geerassociation.org/GEER_Post%20EQ%20Reports/Italy_2009/Cover_Italy2009_Rev.html. Accessed 30 October 2010

Grasso S, Maugeri M (2006) Using K_D and V_s from Seismic Dilatometer (SDMT) for evaluating soil liquefaction. Flat Dilatometer Testing. In: Proceedings of 2nd international conference on the Flat Dilatometer, Washington DC, pp 281–288. http://www.insitusoil.com/docs/Using_KD_and_Vs_from_seismic_dilatometer_for_evaluating_soil_liquefaction.pdf. Accessed 7 November 2010

Harman DE (1976) A statistical study of static cone bearing capacity, vertical effective stress and relative density of dry and saturated fine sands in a large triaxial test chamber. MSc Thesis, Univ. of Florida

Idriss IM, Boulanger RW (2004) Semi-Empirical Procedures for Evaluating Liquefaction Potential During Earthquakes. In: Doolin et al (eds) Proceedings of 11th ICSDEE & 3rd ICEGE. Berkeley, CA, USA, vol 1, pp 32–56

Il Centro (2009) http://ilcentro.gelocal.it/dettaglio/valle-peligna-piccoli-vulcani-del-sisma-dopo-la-grande-scossa-sorti-strani-crateri/1625754. Accessed 27 October 2010

INGV Istituto Nazionale di Geofisica e Vulcanologia (2009) The L'Aquila seismic sequence—April 2009. http://portale.ingv.it/primo-piano-1/news-archive/2009-news/april-6-earthquake/copythe-l-aquila-seismic-sequence-april-2009/view?set_language=en. Accessed 30 October 2010

ISSMGE Technical Committee for Earthquake Geotechnical Engineering—TC4 (1999) Manual for zonation on seismic geotechnical hazards. The Japanese Society of Soil Mechanics and Foundation Engineering

ISSMGE Technical Committee for Ground Property Characterization from In Situ Tests—TC16 (2001) The Flat Dilatometer Test (DMT) in Soil Investigations. A Report by the ISSMGE Committee TC16. Reprinted in Flat Dilatometer Testing. In: Proceedings of 2nd international conference on the Flat Dilatometer, Washington, DC, pp 7–48

Iwasaki T, Tokida K, Tatsuoka F, Watanabe S, Yasuda S, Sato H (1982) Microzonation for soil liquefaction potential using simplified methods. In: Proceedings of 3rd international conference on microzonation, Seattle, vol 3, pp 1319–1330

Jamiolkowski M, Lo Presti DCF, Manassero M (2001) Evaluation of relative density and shear strength of sands from cone penetration test and Flat Dilatometer Test, soil behavior and soft ground construction (GSP 119). ASCE, Reston, Virginia, pp 201–238

Joyner W, Boore D (1981) Peak horizontal acceleration and velocity from strong-motion records including records from the 1979 imperial valley, California, earthquake. Bull Seism Soc Am 71(3):2011–2038

Kulhawy FH, Mayne PW (1990) Manual on estimating soil properties for foundation design. Report EPRI EL-6800, electric power res. inst. Palo Alto, pp 306

Kuribayashi E, Tatsuoka F (1975) Brief review of liquefaction during earthquakes in Japan. Soils Found 15(4):81–92

Leon E, Gassman SL, Talwani P (2006) Accounting for soil aging when assessing liquefaction potential. J Geotech Geoenv Eng ASCE 132(3):363–377

Marchetti S, Monaco P, Totani G, Marchetti D (2008) In Situ Tests by Seismic Dilatometer (SDMT). From research to practice in geotechnical engineering (GSP 180), ASCE, Reston, Virginia, pp 292–311

Maugeri M, Monaco P (2006) Liquefaction potential evaluation by SDMT. Flat Dilatometer Testing. In: Proceedings of 2nd internatinal conference on the Flat Dilatometer, Washington DC, pp 295–305

MedNet (2009) Mediterranean very broadband seismic network—regional centroid moment tensors. http://earthquake.rm.ingv.it/data_id/2206496920/event_out.php. Accessed 30 October 2010

Monaco P, Marchetti S, Totani G, Calabrese M (2005) Sand liquefiability assessment by Flat Dilatometer Test (DMT). Proc XVI ICSMGE, Osaka, 4:2693–2697

Monaco P, Marchetti S (2007) Evaluating liquefaction potential by seismic dilatometer (SDMT) accounting for aging/stress history. In: Proceedings of 4th ICEGE, Thessaloniki, Greece

Monaco P, Schmertmann JH (2007) Discussion of "Accounting for soil aging when assessing liquefaction potential" by Leon E. et al. (in J Geotech Geoenv Eng, ASCE, 132(3): 363–377). J Geotech Geoenv Eng, ASCE, 133(9): 1177–1179

Monaco P, Totani G, Barla G, Cavallaro A, Costanzo A, d'Onofrio A, Evangelista L, Foti S, Grasso S, Lanzo G, Madiai C, Maraschini M, Marchetti S, Maugeri M, Pagliaroli A, Pallara O, Penna A, Saccenti A, Santucci de Magistris F, Scasserra G, Silvestri F, Simonelli AL, Simoni G, Tommasi P, Vannucchi G, Verrucci L (2010) Geotechnical aspects of the L'Aquila earthquake. Earthquake geotechnical engineering, satellite conference, XVIIth international conference soil soil mechanics and geotechnical engineering, vol 10, pp 2–3 2009, Alexandria, Egypt

NEID (2010) National Research Institute for Earth Science and Disaster Prevention, Digital strong-motion seismograph network KiK-net. http://www.kik.bosai.go.jp/kik/index_en.shtml. Accessed 30 October 2010

NTC (2008) Approvazione delle nuove norme tecniche per le costruzioni. Gazzetta Ufficiale della Repubblica Italiana, n. 29 del 4 febbraio 2008—Suppl. Ordinario n. 30, http://www.cslp.it/cslp/index.php?option=com_docman&task=doc_download&gid=3269&Itemid=10. Accessed 30 October 2010

Okada Y, Kasahara K, Hori S, Obara K, Sekiguchi S, Fujiwara H, Yamamoto A (2004) Recent progress of seismic observation networks in Japan —Hi-net, F-net, K-NET and KiK-net—. Earth Planets Space 56:25–28

PIANC (2001) Seismic design guidelines for port structures. Working Group no. 34 of the Maritime Navigation Commission, International Navigation Association, Balkema, Lisse, 474 pp

Robertson PK, Wride CE (1998) Evaluating cyclic liquefaction potential using the cone penetration test. Can Geot J 35(3):442–459

Sabetta F, Pugliese A (1987) Attenuation of peak horizontal acceleration and velocity from Italian strong-motion records. Bull Seism Soc Am 77(5):1491–1513

Santucci de Magistris F (2006) Liquefaction: a contribution to the Eurocode from the Italian guideline "Geotechnical aspects of the design in Seismic Areas. ISSMGE ETC-12 workshop, NTUA Athens, Greece. http://users.ntua.gr/gbouck/etc12/Genera_Report%20_Proceedings_of_the_Athens_Workshop_2006b.pdf. Accessed 30 October 2010

Santucci de Magistris F, Evangelista L (2007) Simplified assessment of the liquefaction susceptibility for the city of Naples, Italy. In: Proceedings of 4th international conference earthq geotechnical engineering thessaloniki, Greece

Santucci de Magistris F, Evangelista L (2010) Some considerations on the 2009 Abruzzo earthquake ground motion. In: Proceedings of 14th European conference on earthquake engineering, Ohrid, Macedonia

Seed HB, Idriss IM (1971) Simplified procedure for evaluating soil liquefaction potential. J Soil Mech Found Div, ASCE 97(9):1249–1273

Trifunac MD, Brady AG (1975) A study on the duration of strong earthquake ground motion. Bull Seism Soc Am 65:581–626

Tsuchida H (1970) Prediction and countermeasure against the liquefaction in sand deposit. Abstract of the seminar, Port and Harbor Research Institute, Yokusuka, Japan (in Japanese)

Utsu T (1982) Relationships between earthquake magnitude scale. Bull Earthq Res Inst 57:465–497 (in Japanese)

Wakamatsu K (1991) Maps for historic liquefaction sites in Japan. Tokai University Press. Japan, 341 pp (in Japanese)

Wakamatsu K (1993) History of soil liquefaction in Japan and assessment of liquefaction potential based on geo-morphology. Ph.D. Thesis. Waseda University, Tokyo, Japan

Working Group ITACA (2010) Data Base of the Italian strong motion data. http://itaca.mi.ingv.it. Accessed 27 October 2010

Working Group UNISANNIO—CIMA–DIGA (2009) Rapporto preliminare sugli effetti indottisull'ambiente fisico dalla sequenza sismica dell'aquilano—ver.1.5. http://www.reluis.it/doc/pdf/Aquila/UniSANNIO_CIMA_UniNA_Report_v1.5.pdf. Accessed 30 October 2010

Yasuda S, Morimoto I, Kiku H, Tanaka T (2004) Reconnaissance report on the damage caused by three Japanese earthquakes in 2003. In: Doolin et al. (eds) Proceedings of 11th ICSDEE and 3rd ICEGE, Berkeley, CA, USA, vol 1, pp 14–21

Youd TL et al (2001) Liquefaction resistance of soils: summary report from the 1996 NCEER and 1998 NCEER/NSF workshops on evaluation of liquefaction resistance of soils. ASCE J Geot Geoenviron Eng 127(10):817–833